Molecular Crystals and Liquid Crystals
Publication details, including instructions for authors and subscription information:
http://www.tandfonline.com/loi/gmcl16

# Cholesteric Blue Phases in Mixtures and in an Electric Field

P. L. Finn [a] & P. E. Cladis [a]
[a] Bell Laboratories, Murray Hill, New Jersey, 07974
Version of record first published: 14 Oct 2011.

To cite this article: P. L. Finn & P. E. Cladis (1982): Cholesteric Blue Phases in Mixtures and in an Electric Field, Molecular Crystals and Liquid Crystals, 84:1, 159-192

To link to this article: http://dx.doi.org/10.1080/00268948208072138

*Mol. Cryst. Liq. Cryst.*, 1982, Vol. 84, pp. 159–192
0026-8941/82/8401-0159 $06.50/0

Printed in the United States of America



# Cholesteric Blue Phases in Mixtures and in an Electric Field

P. L. FINN and P. E. CLADIS

*Bell Laboratories, Murray Hill, New Jersey 07974*

We have determined phase diagrams (using the light microscope) and pitch (using a wedge geometry) for cholesteryl propionate mixed with various nematics and a chiral nematic mixed with cyanohexyloxybiphenyl (6OCB). We have succeeded in untwisting both blue phases, BPI and BPII of the latter mixture in an electric field. We find that with increasing field, BPI transforms to a cholesteric whereas BPII transforms to a nematic before aligning in the field. Furthermore, the voltage to align the blue phases is not very different from that in the cholesteric phase despite the fact that the pitch is quite different in each case.

Our model is that blue phases are triggered by the appearance of submicroscopic isotropic regions in the cholesteric. These regions necessitate nematic boundary conditions at the isotropic interface. Because cholesterics and nematics are thermodynamically the same phase (they are completely miscible), a cholesteric-isotropic emulsion occurs to minimize the loss in twist energy. The nematic is the emulsifier, the inside phase is isotropic and the outside phase is cholesteric. The size of the isotropic regions scales with the square of the pitch. This implies the existence of a maximum cholesteric pitch for which an emulsion solution is possible. This is BPI. We speculate that it is stabilized by the entropy of disclination loops. Increasing temperature results in the emulsion turning inside out so that the cholesteric is now the inside phase and the isotropic liquid the outside one. This is BPII.

A particular example of this model correctly predicts relative periodicities between the cholesteric phase and the blue phases, as well as the maximum pitch of the cholesteric with a blue phase. It also accounts for our observation of blue phases in an electric field and the habits of materials with both positive and negative dielectric anisotropies in the Cano wedge.

## I INTRODUCTION

### A Historical

Even though the cholesteric blue phase was one of the first manifestations of liquid crystallinity ever observed,[1] its structure has yet to be elucidated. The main features of blue phases (BP) are:

1. They occur in a very narrow temperature range (typically on the order of a half a degree) between the cholesteric liquid crystal and isotropic liquid phases. The entropy change at the cholesteric-BPI and BPI-BPII transitions are very small.[2] Most of the entropy change is at the blue phase to isotropic transition.

2. There are two three-dimensionally ordered blue phases called BPI and BPII[3] and a third amorphous blue phase called BPIII or the blue fog.[1,4] They all occur in the half degree temperature range below the isotropic transition.

BPI seems to be frequently a b.c.c. structure,[3,5-7] but Nicastro and Keyes have found that short pitch favors a non-cubic structure, intermediate pitches the f.c.c. and long pitch the b.c.c. or simple cubic latttice.[6] In at least one mixture, BPII has been found to be simple cubic.[7]

3. Transitions from cholesteric to BPI, BPI to BPII and BPII to BPIII are discontinuous.[1,2,8] The BPIII to isotropic transition may be continuous.[8]

4. Blue phases selectively reflect circularly polarized light; there's a small half-width to the reflection bands and the wavelength reflected depends on the angle of reflection—as in Bragg reflection. There are discontinuities in the optical activity at the cholesteric to BPI and BPI to BPII transitions.[9] The periodicity of BPI and BPII are red shifted with respect to the cholesteric state. Sometimes, the periodicity of BPI is longer than BPII and sometimes, it is not.

5. Frequently there is no birefringence but some evidence of birefringence has been observed in some compounds.[10]

6. There is an upper limit to the pitch of cholesterics exhibiting the blue phase.[1,6]

Recently, Brazovskii,[11] wrote the cholesteric energy in the form:

$$F_{\text{chol}} = F_0 + \tfrac{1}{2} Q^2[a + f_{\text{el}} - K_2 q_0^2] - bQ^3 + cQ^4 \tag{1.1}$$

where $a = a_0(T - T^*)$ and

$$2f_{\text{el}} = K_1(\text{div}\mathbf{n})^2 + K_2(\mathbf{n}\cdot\text{curl}\mathbf{n} + q_0)^2 + K_3(\mathbf{n}\times\text{curl}\mathbf{n})^2 + \text{surface terms}, \tag{1.2}$$

where $\mathbf{n}$ is the director and $q_0$ is the inverse pitch, $K_1$, $K_2$ and $K_3$ are the Frank constants and $\mathbf{Q}$ is the traceless part of the dielectric tensor,

$$\mathbf{Q} = Q[\mathbf{nn} - \tfrac{1}{3}\mathbf{I}] \tag{1.3}$$

where $\mathbf{I}$ has elements $\delta_{\alpha\beta}$.

Comparing the energy of Eq. 1.1 to that of a nematic whose transition temperature to the isotropic phase is $T_{NI} = T^* + b^2/4a_0c$, deGennes[12] points out that (1.1) implies for the cholesteric to isotropic liquid transition temperature, $T_{CI}$,

$$T_{CI} = T_{NI} + \frac{K_2 q_0^2}{a_0} \tag{1.4}$$

so that there is a temperature range $(T_{CI}, T_{NI})$ whose width is proportional to $q_0^2$ where the normally "uniaxial" cholesteric becomes "biaxial"—or something

equally strange occurs. In agreement, the blue phase temperature range will be seen to broaden as the pitch gets shorter. Brazovskii found that a hexagonal arrangement of twist axis could result in a smaller effective coefficient for the cubic term but a larger coefficient for the quartic term so that once $Q$ became smaller than some particular value, this hexagonal type structure would occur. In fact Sigaud[13] pointed out that some of the blue phase platelets grew in a hexagonal habit. Alexander[12] and Hornreich and Shtrikman[14] favor a b.c.c. structure because this reduces the cubic term more than the hexagonal array and indeed, this has frequently been observed to be the case.[3-7]

Kuczynski *et al.*[15] have proposed a conical cholesteric as a specific model for one of the blue phases—that is, the director (the direction of long range orientational ordering) is not perpendicular to the twist axis but is inclined at some angle to it. By suitably picking the angle, they account for the optical isotropy as well as the cholesteric-like reflection properties.

### B Outline of our model

In this paper, we propose that blue phases result from the spontaneous emulsification of the isotropic liquid by the cholesteric liquid. The configuration of the cholesteric liquid is disclination loops rather regularly arranged with nematic and isotropic regions filling up the spaces. The nematic is a kind of emulsifier which exists at the interface between cholesteric and isotropic liquid where a uniform director orientation is required. Experimental support for the nematic presence in the blue phase is our observation of the characteristic "twinkling" associated with the nematic phase in BPII.

Facts which militate in favor of this description are:

1. Nematics and cholesterics are not thermodynamically distinct thus are infinitely miscible. In order to maximize the nematic—cholesteric mixing entropy, the interface between the cholesteric and nematic will be maximum. This drives the cholesteric to occupy the smallest volume consistent with its twisted symmetry but which renders it more nematic-like. We propose for its director configuration, a non-singular disclination loop: in BPI the radius is the half pitch since topologically this minimizes the twist energy; in BPII, the cholesteric is contained in a sphere of radius on the order of a quarter of a pitch. This constraint makes it energetically more feasible for the director configuration to be untwisted in order to fulfill the nematic-like boundary conditions at the sphere interface.

A similar nematic-cholesteric mixing could occur in the bubble domain texture.[16] In this case, the nematic phase is induced by rigid boundary conditions or an external field. An example of this is shown in Figure 1. In Figure 1, the bubble domain texture is induced in cholesteryl propionate by applying 425 volts dc to a 76 $\mu$m sample.

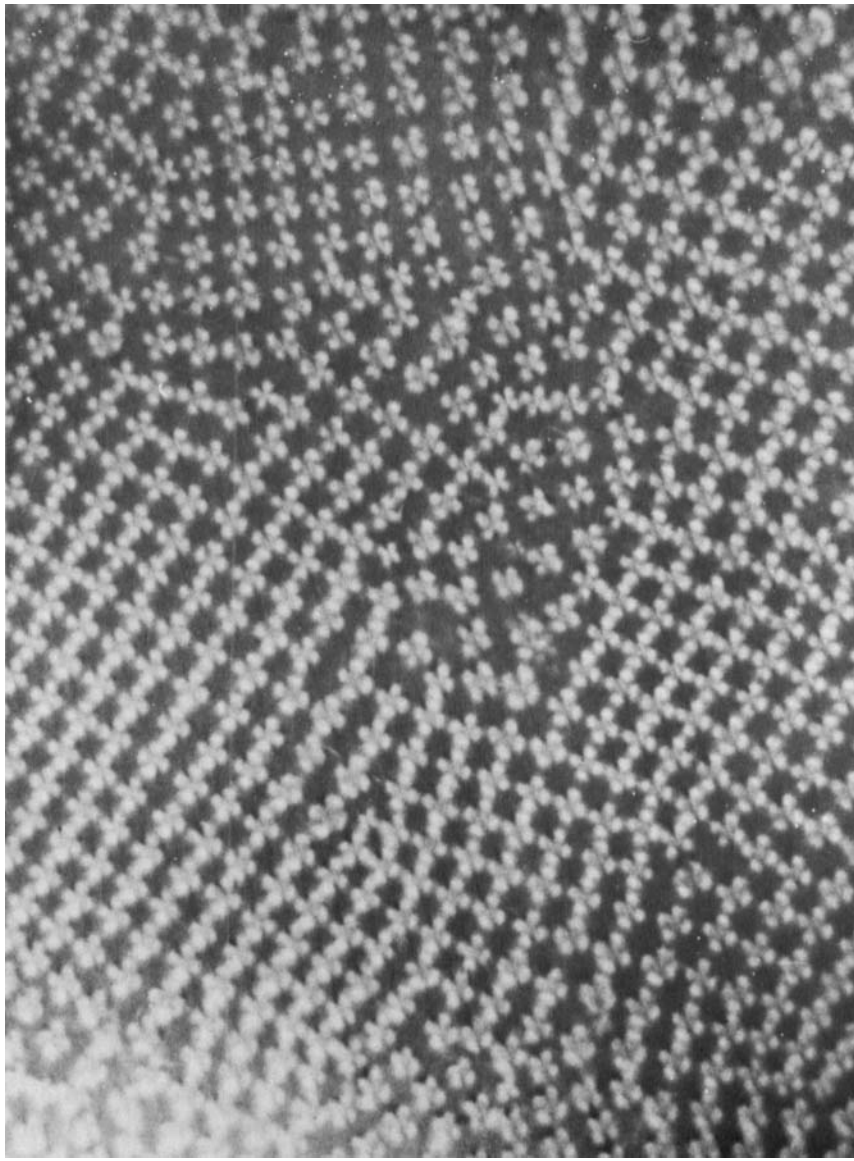

FIGURE 1 The bubble domain texture induced in cholesteryl propionate. The sample is contained in a 76 micron thick cell. The average size of the bubbles is ~30 microns. The applied voltage is 425 volts dc. The cells are blurred somewhat because they are in motion and because there are actually two layers of bubbles—one in the top half and the other the bottom half of the sample.

Figure 1 demonstrates a case where nematic and cholesteric regions are forced to coexist. Rather than segregrate into a macroscopic nematic region and a macroscopic cholesteric region, the system "emulsifies" so that the two manifestations of the same phase are as well mixed as possible and the total loss in twist energy is minimum. And, of course, when a cholesteric is reduced to a sphere the size of its pitch, it's more a nematic than it is a cholesteric.[17]

In Figure 1, we have induced the nematic phase with an electric field. In the blue phase, it is done by isotropic regions appearing in the cholesteric near the clearing temperature.

2. In the nematic regions, the cholesteric will lose twist energy $\sim[K_2q^2$ (volume of nematic)]. In order to minimize this, the nematic volume will be minimum or the isotropic volume will be maximum. But, there is a positive interfacial energy at the nematic isotropic interface and in order to minimize this, the nematic-isotropic surface area will be minimum. These two competing effects result in an isotropic region of radius, $R_{NI}$, which scales with the pitch squared. When $R_{NI}$ is on the order of the half-pitch, then clearly, the emulsion can no longer occur. Our estimate of when this occurs agrees very well with the cases we have studied in detail. (See Section IV C3).

3. To create the isotropic region in the first place requires $[(L/T_{CI})\Delta T \times$ volume of isotropic region] energy units, where $L$ is the latent heat and $T_{CI}$ the transition temperature. Minimizing this with the twist energy results in the prediction that the blue phase range $\Delta T < K_2q^2/2(L/T)$. Again this estimate seems to agree rather well with the evidence. (See Section IV C3).

The term nematic will now refer specifically to regions of zero twist and cholesteric to regions of non-zero twist.

The following sequence of events is envisaged: In the vicinity of the isotropic phase, an isotropic seed forms in the cholesteric. Nematic coats this interface. Because cholesteric and nematic phases are not thermodynamically distinct, their interfacial energy is essentially negative. The cholesteric nematic interface is unstable and increases in area.

The size of the isotropic regions will be determined by the competition between the gain in twist energy and the loss in surface energy. For small enough pitch this will be much smaller than the pitch so that the isotropic liquid becomes dispersed in the cholesteric matrix. In the language of emulsions, the "inside phase" is isotropic and the "outside phase" is cholesteric. This we propose is BPI. It is depicted in the top of Figure 2.

As the temperature increases, the size of the isotropic regions increases until eventually the cholesteric spheres are attached only by nematic links (middle Figure 2) which eventually break so that the isotropic liquid is now the outside phase and the cholesteric is the inside phase (bottom Figure 2). The emulsion has turned itself inside out. The inside phase is now untwisted cholesteric and

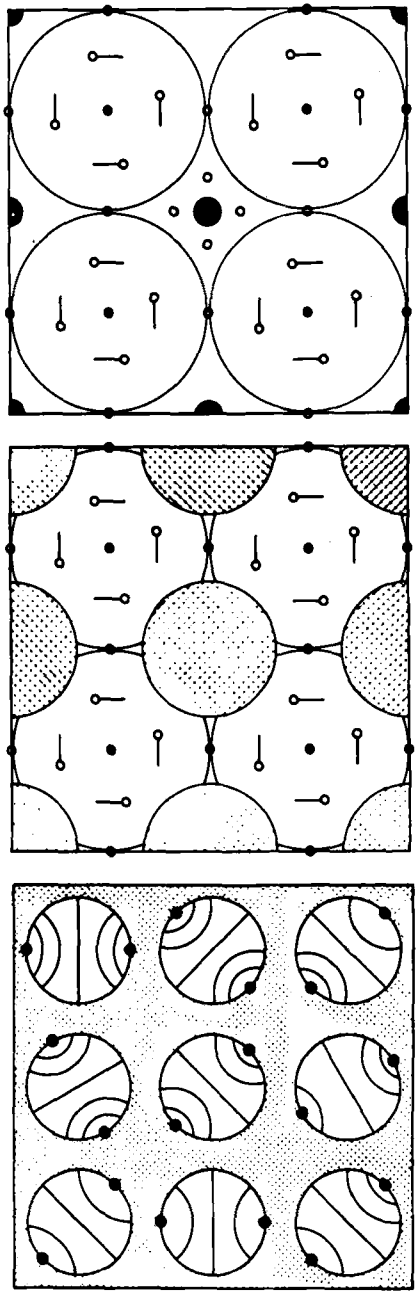

the outside phase is isotropic. This we propose is BPII. This kind of model predicts a viscosity anomaly at the BPI-BPII transition, as well as at the BP-isotropic transition.

When the distance between the spheres becomes so large that there are no long range positional correlations, we have the blue fog or BPIII.

An emulsion theory such as this one is consistent with the extremely narrow temperature range over which blue phases are stable.

Because our model is based on spherical units arranged in various space filling configurations, it is not unlike the way opals are formed.

Basically our model is that the blue phase is an array of non-singular disclination loops. In general, these defects may even be singular but we do not consider that case here. In this respect it is similar to the one proposed by Saupe[18] although the details differ. Furthermore, our model is not inconsistent with the theory of Brazovskii although again, the details differ. The factor determining the stability of our lattice of defects is speculated to be the entropy of disclination loops combined with the elastic energy and pitch of the cholesteric phase.

Our study has been primarily in mixtures where two phases can co-exist. This cannot occur in a pure compound for which blue phases have been observed. We rationalize this by assuming that even the purest of organic materials has some impurities and indeed impurities which decrease the pitch increase the range of the blue phases—at least initially. An exception to this is provided by the chiral nematic mixtures. Although the pitch steadily increases with increasing concentration of a nematic, the blue phase range first increases then decreases. Another rationale would be that the uniform dispersion of one phase inside another is a new distinct phase and is not coexistence of two macroscopic phases. Thus, it could occur even in the purest compound. In our model, this would seem to exclude the occurrence of BPII in an ultra pure material although BPI would still be possible.

The observations and experiments which led us to this picture are presented

FIGURE 2 Schematic of our model of the blue phases. In the top figure we are viewing the equatorial sections of spheres. The spheres are arranged in a square lattice in the plane. In the top figure, at the points of contact both the director and twist axis coincide. The cross hatched areas are small regions of isotropic liquid. Between the spheres are nematic regions. This is our model of BPI.

In the middle scheme, the isotropic regions have grown and begun to eat into the cholesteric regions.

In the bottom scheme, the isotropic regions have taken over and each spherulite is now effectively untwisted cholesteric (shown in diameter section only) whose orientation is randomized by Brownian motion (shown only in two dimensions in the figure). This is our model of BPII, a kind of plastic crystal of spherulites free to rotate in three-dimensions. But, in order to account for the optical rotatory power of BPII the axis of each sphere may be systematically twisted with respect to each other.

in Sections II and III. We have determined the phase diagram and pitch for a variety of compounds and have succeeded in untwisting both BPI and BPII in one mixture of large positive dielectric anisotropy. Details of the model are presented in Section IV.

## II SAMPLES AND SAMPLE PREPARATION

### A Samples

The materials are shown in Table I. The nematic materials were chosen because they represented a variety of dielectric anisotropies, $\epsilon_a = \epsilon_\parallel - \epsilon_\perp$, ranging from $-4$ for S1014 to $+12$ for M18 and M24. Since our primary hypothesis is that the blue phase is a defect model, then presumably it would be sensitive to

TABLE I

The compounds used in this study. In the left hand column are acronyms for the compounds, in the middle their chemical name and on the right their formula. In this paper we present data for cholesteryl propionate mixed with the first four nematics, M-18 with CB15 and CE2 mixed with S-1014. The pitch of CE1 is too large for it to exhibit the blue phase phenomena.

| | | |
|---|---|---|
| | NEMATIC | |
| S-1014 | 2-CYANO-4-HEPTYLPHENYL 4'-PENTYL BIPHENYL-4-CARBOXYLATE | 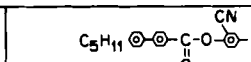 |
| CBOOA | N-(4-CYANOBENZYLIDENE)-4-N-OCTYLOXYANILINE | 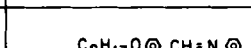 |
| 2-7AOB | 4,4'-DIHEPTYLOXYAZOXYBENZENE | 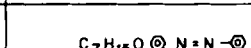 |
| M-24 | 4-CYANO-4'-N-OCTYLOXYBIPHENYL | 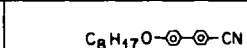 |
| M-18 | 4-CYANO-4'-N-HEXYLOXYBIPHENYL | 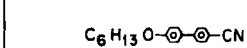 |
| | CHOLESTERIC | |
| CP | CHOLESTERYL PROPIONATE | 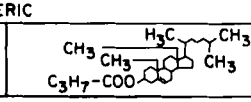 |
| | CHIRAL NEMATICS | |
| CE 1 | 4-CYANOPHENYL 4'-(2-METHYLBUTYL) BIPHENYL-4-CARBOXYLATE | 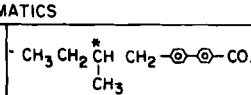 |
| CE 2 | 4-(2-METHYLBUTYL) PHENYL 4'-(2-METHYLBUTYL) BIPHENYL-4-CARBOXYLATE | 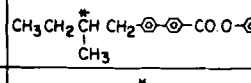 |
| CB 15 | 4-CYANO-4'-(2-METHYL) BUTYLBIPHENYL | 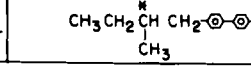 |

the specific boundary condition of the director at the isotropic-cholesteric interface. Empirically, we have observed that large positive dielectric anisotropies (as in M24 and M18) tend to orient with the director parallel to the interface normal (homoeotropically) whereas the negative ones tend to orient in the plane of the interface so that there is no net polarization vector in the interface. These different boundary conditions set-up different defect arrays providing a clue to the blue phase structure. A consequence is the different habits for monocrystals of blue phase when homogeneous boundary conditions are imposed.

The chiral nematics also exhibit blue phases when their pitch is small enough. In particular, CB15 has only one blue phase at −28°C. CB15 was chosen because of its large positive dielectric anisotropy (and small pitch) and was used in mixtures with M18 (6OCB) in the electric field experiments where we unwind the blue phase.

The blue phase of cholesteryl propionate had been studied by Gusakova and Chystiakov[19] who deduced that the pitch of its blue phase must be outside the visible range, but became visible when mixed with a nematic. Our supply of cholesteryl propionate: the stocks supplied by Eastman Kodak, Aldrich and van Schuppen (presumably ultra pure) all exhibited blue phases, although their range could be considerably extended when mixed with a nematic. Yet, the transition temperature of our stocks of CP was generally 112°C–113°C, whereas that of Chystiakov and Gusakova is ~116–117°C, i.e., apparently much purer.

### B Sample preparation

Samples were (1) sealed inside flat glass capillaries for phase diagram studies; (2) sandwiched between a cylindrical lens and flat for pitch measurements and (3) sealed between parallel glass plates coated with indium-tin-oxide electrodes.

Mixtures were made by weighing each component then mixing them in the isotropic state for one hour in vacuum. The sample cells which were to be sealed were filled in vacuum and the fill hole subsequently sealed. The flat glass capillaries, .1 × 1 mm, were mounted on glass slides and the phase diagrams determined by light microscopy and a Mettler hot stage. Before any measurements were made, the sample was left in the isotropic state for one hour. In this way we obtained well mixed samples with reproducible transition temperatures.

The Cano Wedge[22] samples were treated with a surfactant (a weak solution of polyvinyl alcohol or ACM-72 available from Atomergic) to promote homogeneous alignment, then rubbed. These samples were not sealed. The radius of curvature of the cylindrical lens is 20 mm. The defect lines (also called Cano lines) mark the change in thickness of the wedge in units of the half-pitch. Their separation was measured using a traveling hair eye-piece and the light microscope. Even in unsealed samples, the chiral nematics and biphenyls were stable when left over night at the BPI-BPII transition.

## III OBSERVATIONS

### A Mixtures of cholesteryl propionate and nematics

Figure 3 shows the temperature versus concentration plots for mixtures of various nematics with cholesteryl propionate (CP). The two upper compounds (negative dielectric anisotropy) tend towards ideal behavior whereas the two bottom compounds show an eutectic type behavior. The initial effect of the nematic on the blue phase (Figure 4) is to broaden the blue phase temperature range. This trend does not always persist to higher concentrations where the pitch becomes large. 2-7AOB shows the greatest effect here, with S1014 second, CBOOA third and M-24 last. This correlates with the absolute magnitude of the pitch at any given concentration (Figure 5). The 2-7AOB mixtures have the smallest pitch, the widest blue phase and form nearly ideal mixtures. M24 has the narrowest blue phase, the longest pitch and the most eutectic phase diagram.

Figure 6 shows the maximum half-pitch of the cholesteric phase which forms a blue phase as a function of dielectric anisotropy of the nematic. The dielectric anisotropy of 2-7AOB is $-.02$,[19] of CBOOA is 5.5,[21] M24 is 12 and S1014, $-4$.

We hope to check both these points in the future.

### B Mixtures of chiral nematics and nematic

*1 Phase diagram and pitch measurements* Figure 7 shows the (a) phase diagram, (b) the blue phase width and (c) the pitch of CB15 and M18 (6OCB) mixtures as a function of concentration. With such a large temperature range, the blue phase transitions are not observable on the Figure. In Figure 7(b) we observe the familiar effect that the blue phase range initially increases with increasing concentration of 6OCB (M-18) then decreases as the pitch increases. No blue phase is observed in mixtures containing 80% or more of 6OCB. In (a) and (b) only the temperatures and blue phase range on increasing temperatures are shown. Unlike the cholesteryl propionate mixture, the pitch dependence of this mixture is linear. We were not able to measure the half-pitch of pure CB15 but estimate it by extrapolation to be 650Å.

Figure 8 shows the half-pitch versus temperature for the 50% mixture as measured by the Cano wedge[22] in the cholesteric, BPI and BPII phases. Figure 9 shows the same thing for 34.5% CE2 in S1014. Figure 8 is a mixture with positive dielectric anisotropy and we shall discuss its behavior in a large electric field next. Figure 9 is a mixture of negative dielectric anisotropy. In the positive mixture, the periodicity of BPI is less than the periodicity of BPII. This is reversed in the negative case. We attribute this to the different habits of the two materials in a homogeneously oriented sample (Section IVE).

The periodicity measured in the Cano wedge corresponds to the wavelength of the center of the Bragg reflection. For example, for the sample shown in Figure 9, the reflection band extends from 516 nm to 485 nm for BPII. This

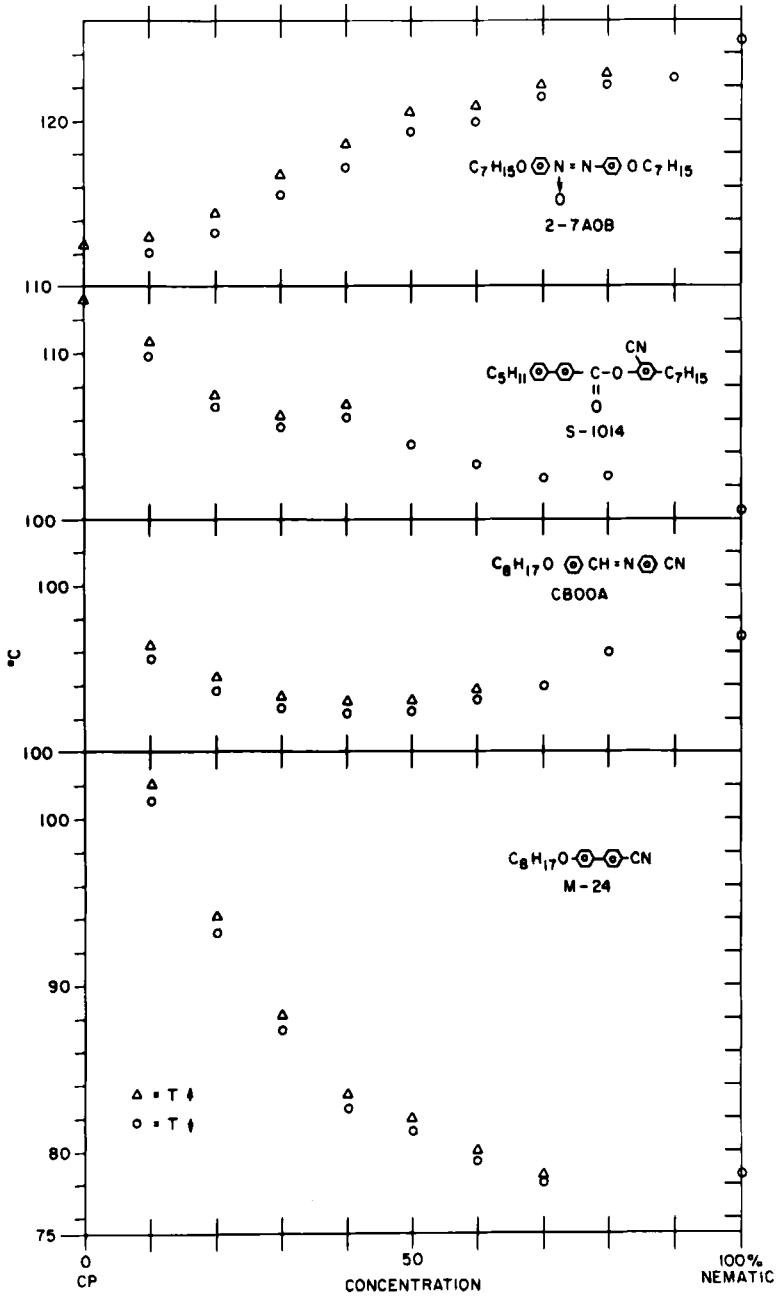


FIGURE 3 The blue phase to isotropic transition temperature for mixtures of cholesteryl propionate with four different nematics on both increasing and decreasing temperature. In the top two figures, the transition line is nearly linear (ideal) whereas the bottom two are of the eutectic type—i.e., non-linear. The top two nematics have negative dielectric anisotropy, the bottom two, positive.

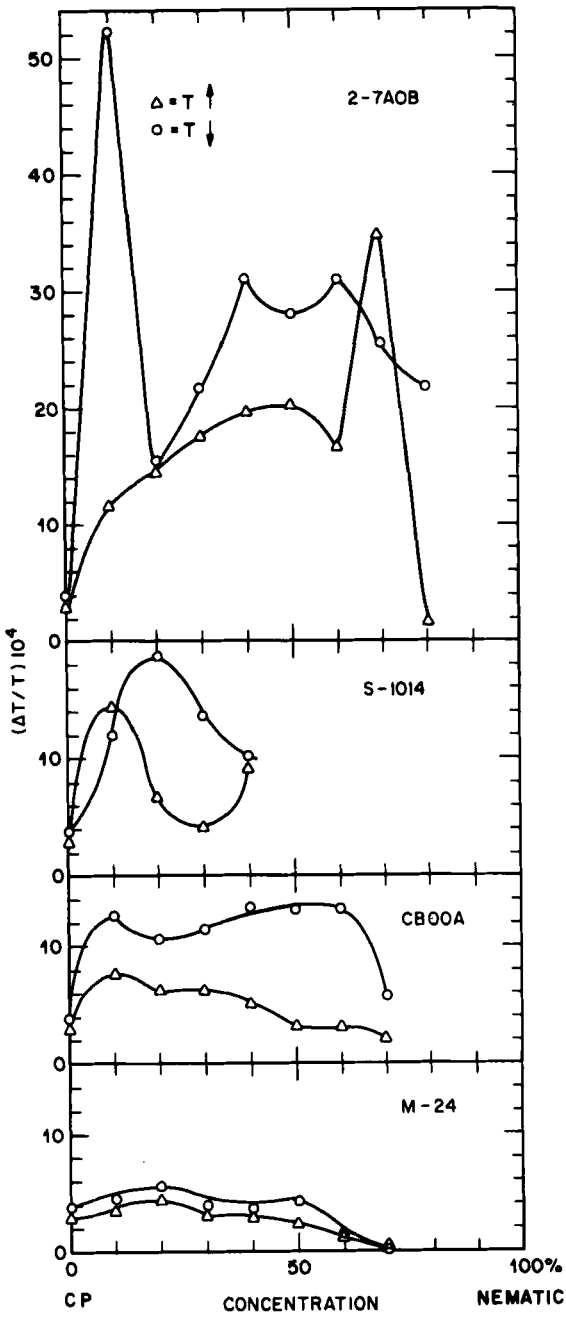


FIGURE 4 The width of the blue phase region normalized to the BPII-isotropic transition temperature (in °K). In every case the addition of a small amount of nematic increases the temperature range of the blue phase. This is most dramatic when CP is mixed with 2-7AOB and least with the M-24 mixture even though the magnitude of the transition temperature is smaller in this latter case.

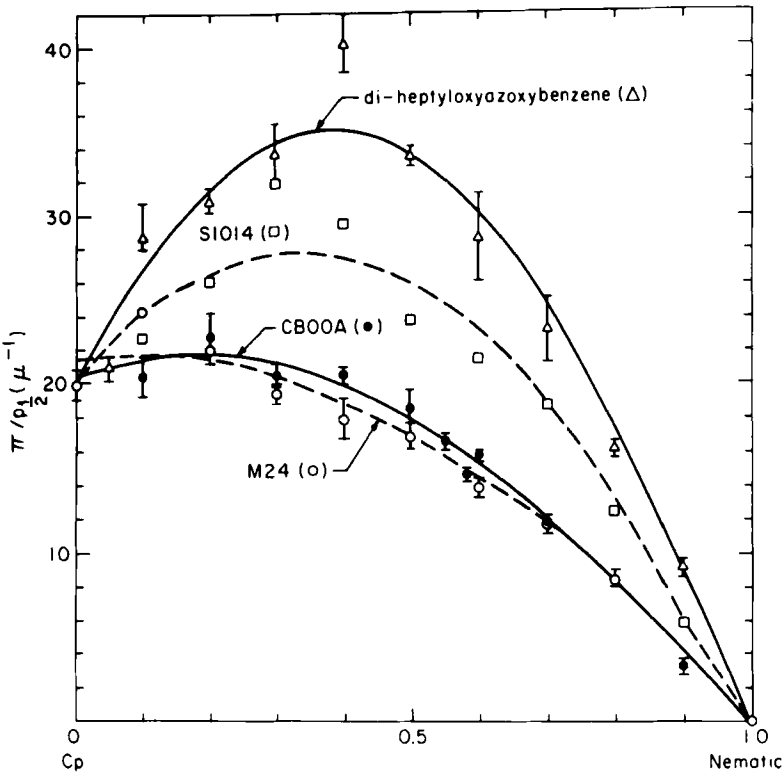


FIGURE 5 The inverse of the half-pitch times $\pi$ versus concentration of the nematics shown in Figure 4. A comparison of Figure 4 with this figure shows that the broadest blue phase occurs for the shortest pitches.

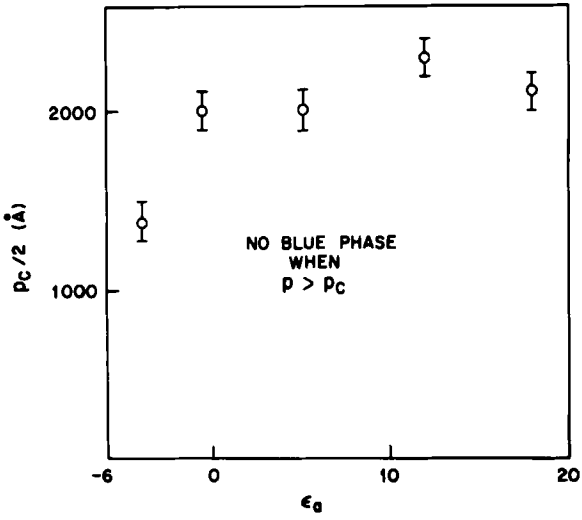


FIGURE 6 The maximum half-pitch of the cholesteric phase which exhibits a blue phase versus the dielectric anisotropy of the nematic mixed with cholesteryl propionate.

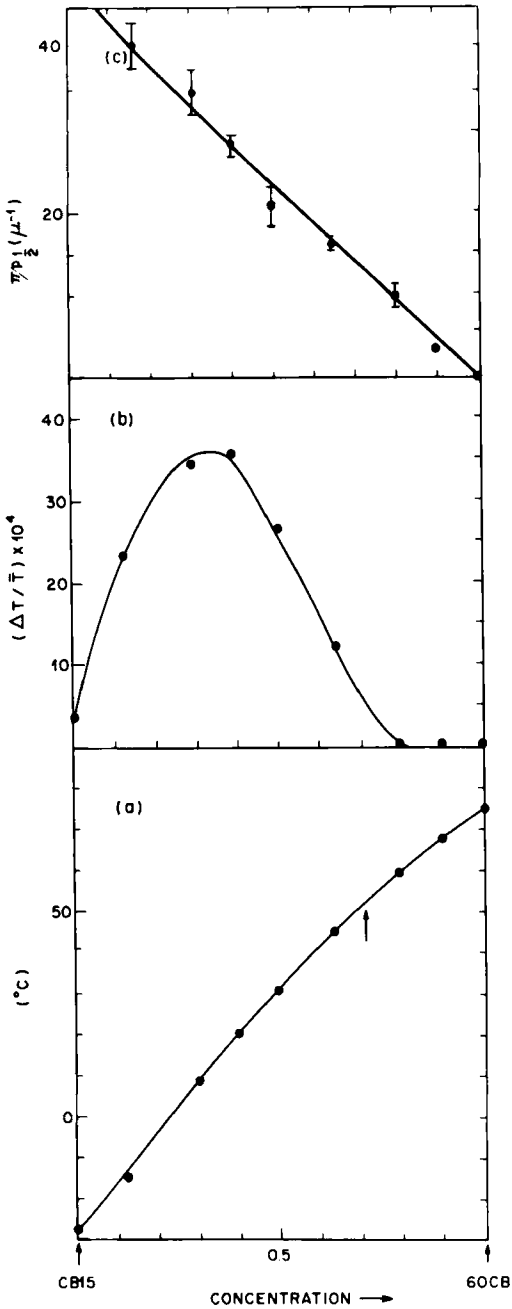


FIGURE 7 Transition temperatures (a) blue phase widths (b) and inverse half-pitch versus concentration (c) of 6OCB (M18) in CB15. Unlike the compounds discussed in Figures 3–6, the inverse half-pitch times $\pi$ versus concentration is linear. The transition temperature versus concentration is nearly linear (7a). As in Figure 4, the range of the blue phase is initially increased with small concentrations of nematic (M18). When the half-pitch becomes greater than ~1000Å, it decreases. When the half-pitch exceeds 2600Å, no more blue phases are observed.

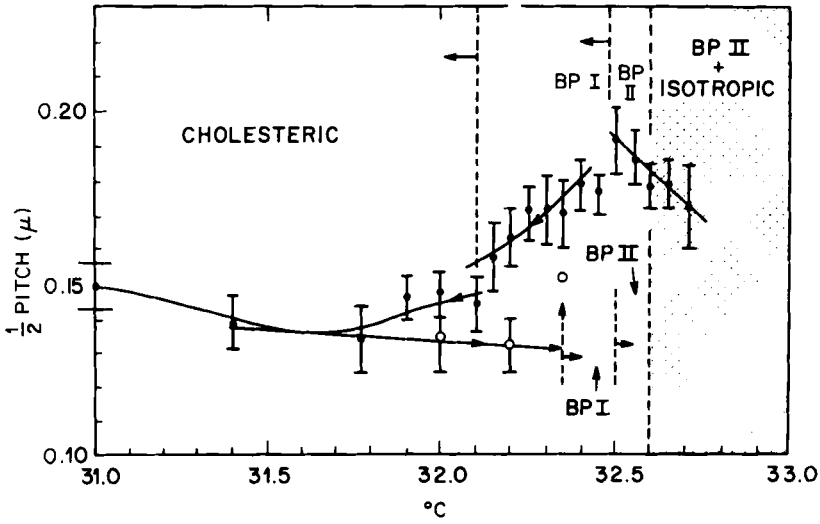


FIGURE 8 Pitch versus temperature for the 50% CB15-6OCB (M18) mixture as measured in the Cano wedge. Between ten and fifty Cano lines are observed and measured at each temperature. The periodicity of the Cano lines corresponds to a change in thickness equivalent to the half-pitch in the cholesteric phase. This mixture has positive dielectric anisotropy.

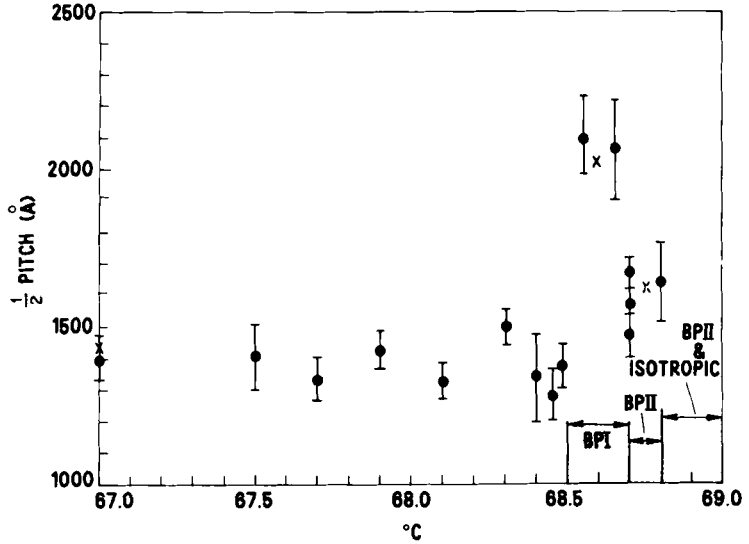


FIGURE 9 Half-pitch versus temperature for 34.5% S1014 in CE2. This mixture has negative dielectric anisotropy. Note in this figure and Figure 8, the very large blue phase-isotropic region observed.

corresponds to a half-pitch measuring 161.8 nm (assuming 1.5 is the index of refraction). This is shown as an $X$ on Figure 9. Similarly, in BPI, this is 207.8 nm and in the cholesteric phase far from the blue phase it is 144.5 nm also shown as $X$'s on Figure 9.

In Figure 8, we found for the center of the corresponding Bragg reflections 481 nm in the cholesteric phase, 512.5 nm in BPI and 568 in BPII. These measurements were made with both increasing and decreasing temperature. The direction of the measurements are shown by the arrows in the figure.

Hysteresis is observed in the pitch and in the BPI-cholesteric transition shown by the appropriate vertical dashed lines. The BPI which nucleated from the cholesteric did not show the Cano lines. They reappeared in BPII. Cooling from BPII to BPI, Cano lines were observed so that a measurement of BPI has only been made in cooling from BPII.

In the region marked (BPII + isotropic), small isotropic droplets co-existed with the blue phase (which is yellow in Figure 8 and greenish in Figure 9). The droplets appeared uniformly first in the thicker part of the wedge then gradually over the whole field of view. They became larger as the temperature increased. They did not coalesce. Although the Cano lines were interrupted by round isotropic islands, they were defined sufficiently well to estimate the pitch.

Sometimes, nematic like "twinkling" was observed in this BPII even when the sample was well enough oriented to give the Cano lines.

In these oriented samples, both BPI and BPII "looked" just like the cholesteric—the whole field of view was uniform in color. This agrees with similar observations made by Kuczynski *et al.*[1,15] that is, homogeneously oriented cholesteric in either of BPI, BPII or the cholesteric phase, except for their color, are identical. In particular, the additional translational ordering of BPI and BPII compared to the cholesteric phase is not obviously apparent.

*2 Periodicity* The periodicity of the uniform cholesteric is $\pi/q_0 = p_0/2$ where $p_0$, the pitch, is the distance for a $2\pi$ rotation of the director. The longest wavelength reflected by a homogeneously oriented cholesteric is

$$\lambda_{\text{chol}} = p_0 n \tag{2.1}$$

where $n$ is the index of refraction $\cong 1.5$.

Assuming a lattice parameter, $a_{\text{BP}}$, for the blue phases, the wavelength of the $(h, k, l)$ reflection will be

$$\lambda_{\text{BP}} = 2a_{\text{BP}} n/\sqrt{h^2 + k^2 + l^2}. \tag{2.2}$$

Thus

$$\left[\frac{\lambda_{\text{BP}}}{\lambda_{\text{chol}}}\right]_{(h,k,l)} = \frac{2a_{\text{BP}}/p_0}{\sqrt{h^2 + k^2 + l^2}}. \tag{2.3}$$

Now,

$$\left[\frac{\lambda_{BPI}}{\lambda_{chol}}\right]_{(2,0,0)} = a_{BPI}/p_0 \tag{2.4}$$

and $a_{BPI}$ is the length of a cube edge. Thus the (2,0,0) reflection relates the size of the BP cubes to $p_0$. This has been found to be close to but larger than one.[5] When this ratio reaches one, BPI transforms to BPII.

The agreement between the periodicity of the cholesteric determined by the Cano wedge with that determined in back reflection, confirms that the Cano wedge measures the half, not the whole, pitch.

Similarly for the blue phases, both methods of measuring the periodicity lead to identical results. In the case of the 6OCB-CB15 mixture (Figure 8), the longest wavelength is a bright rose. This corresponds to the (1,1,0) planes of a b.c.c. lattices say. Since the color this sample shows is blue, we conclude that the homogeneous alignment induces the (2,0,0) planes to orient parallel to the wedge so that

$$\frac{a_{BPI}}{p_0} = 1.25. \tag{2.5}$$

In the CE2-S1014 mixture (Figure 9), the (1,1,0) planes are parallel to the wedge since the longest wavelength is reflected by the sample. Thus,

$$\frac{\lambda_{BPI}}{\lambda_{chol}} = 1.62 = 2a_{BPI}/\sqrt{2p_0} \tag{2.6}$$

and

$$\frac{a_{BPI}}{p_0} = 1.15 \tag{2.7}$$

for this mixture. For these mixtures, then, the cube size is consistently $\sim 1.2p_0$ in BPI when we assume a b.c.c. structure.

In the case of BPII,

$$\frac{\lambda_{BPII}}{\lambda_{chol}} = 1.45 \tag{2.8}$$

for Figure 8 and

$$\frac{\lambda_{BPII}}{\lambda_{chol}} = 1.19 \tag{2.9}$$

for Figure 9.

In this case, the lattice is probably simple cubic.[7] If the (1,0,0) planes orient parallel to the wedge in the 6OCB-CB15 mixture and the (1,1,0) planes in the

S1014 mixture (due to the constraint imposed at the cholesteric isotropic interface as discussed in Section IV E), we get

$$\frac{a_{\mathrm{BPII}}}{p_0} = 0.75 \tag{2.10}$$

in the former case and

$$\frac{a_{\mathrm{BPII}}}{p_0} = 0.84 \tag{2.11}$$

in the latter. Therefore, assuming a simple cubic structure for BPII, the cube edge is $\sim 0.8 p_0$.

These results will be seen to fit our model very well (Section IVC2 and IVD).

*3 Electric field measurements* We unwound the pitch of the cholesteric phase and blue phases of the 50% mixture of CB15 and M-18 (6OCB) by applying either an AC or DC electric field.

The samples were observed in the light microscope as the electric field was applied. They were considered "unwound" when there were no more disclinations in the field of view and the sample, appeared black between crossed polarizers. $n$ is the extraordinary index of refraction which ranges from $n_e$ when the electric vector is parallel to the long molecular axis, to $n_0$ when it is perpendicular to it. Because both these molecules have positive dielectric anisotropy ($\epsilon_a = \epsilon_\parallel - \epsilon_\perp \cong 10$–$12$ cgs), the molecules align parallel to the electric field and in our geometry this is the viewing direction. Once the sample is unwound, $n \equiv n_0$ and the retardation of the sample, $(n - n_0)d$, is zero. This can be checked by the maltese cross formed by the sample in convergent light.

Usually, the electric field generates a circulation in the sample. It is largely for this reason the material must be in a sealed container—otherwise the sample leaks away.

The circulation present in both AC and DC fields, generates many different kinds of instabilities. A variety of textures were associated with these instabilities: some looked like Williams' domains; in another, the domains resembled the convolutions observed in a brain; still another looked like a large ($\sim 100\mu$) hexagonal net. Due to the variety and complexity of these effects, many of which have been investigated by others,[23] we do not discuss them. Suffice it to say, once completely untwisted, the sample looked "homoeotropic" even though there was still circulation.

BPI in this mixture forms large bluish platelets. The stirring motion induced by the applied field makes it look like a furiously boiling, deep blue liquid. Just

before BPI transforms to the cholesteric state, brownish flecks are observed in the roiling blue fluid. These gradually dominate and the sample turns reddish brown entirely. With increasing field, the birefringence increased until the sample turned yellowish. In this regime, many defect lines such as usually observed in large pitch cholesterics are seen. With increasing field, the birefringence of the sample starts to decrease and it turns a whitish-grey, then black when the entire field of view was unwound and the birefringence was once again zero and the maltese cross is seen in the Bertrand lens (conoscope).

When the field was turned off abruptly, the sample became an opaque, featureless, white—like a low-grade opal. Gradually, small bluish disc-like objects condensed out of this opaque fog and slowly grew to form platelets.

BPII "unwound" to first, a nematic-like Schlieren, that is to say, there were none of the lines usually observed in large pitch cholesterics and in the transition texture of BPI. Just before the transition to the nematic-like Schlieren, the sample turned a dull, reddish brown color similar to BPI.

When there were macroscopic isotropic holes in BPII, at low fields, BPII broke down into confetti-like flakes. These churned around in the isotropic liquid and became smaller as the field increased. They eventually disappeared leaving the entire sample isotropic.

In such large fields, a very weak maltese cross is observed in convergent light even in the isotropic phase due to the field induced birefringence.

The average power (uncorrected for power factor) to unwind the cholesteric and the blue phases was found by measuring the RMS voltage and current for a sinusoidal waveform using a digital multi-meter. It depends upon the frequency (Figure 10) and the temperature (Figure 11).

Figure 10 shows a plot of the frequency vs power to unwind a 125$\mu$ sample in BPI ($T = 30.1$°C) and BPII ($T = 30.6$°C) in the 50% CB15-M18 mixture. The dc power to unwind BPI is $1.4 \times 10^{-3}$ watts. The voltage was 702 volts dc. As the frequency decreases, the voltage to unwind decreases until 30 cps. Below 30 cps, the voltage to unwind increases again and the current falls off to microamps.

Figure 10 shows an anomaly in the power vs frequency curve around 1 watt. Since the shift makes the high power end more collinear with a lower temperature curve, heating, although probably present at 1 watt may not be the only factor involved. Perhaps the numerous instabilities are frequency dependent which in turn would affect the impedance of the cell and give rise to the anomaly.

In Figure 11, we plot the dc voltage to unwind the cholesteric, BPI and BPII phases. The interesting result is that the voltage to unwind blue phases is *comparable* to the voltage to unwind the cholesteric phase even though the blue phase reflections correspond to longer wavelengths.

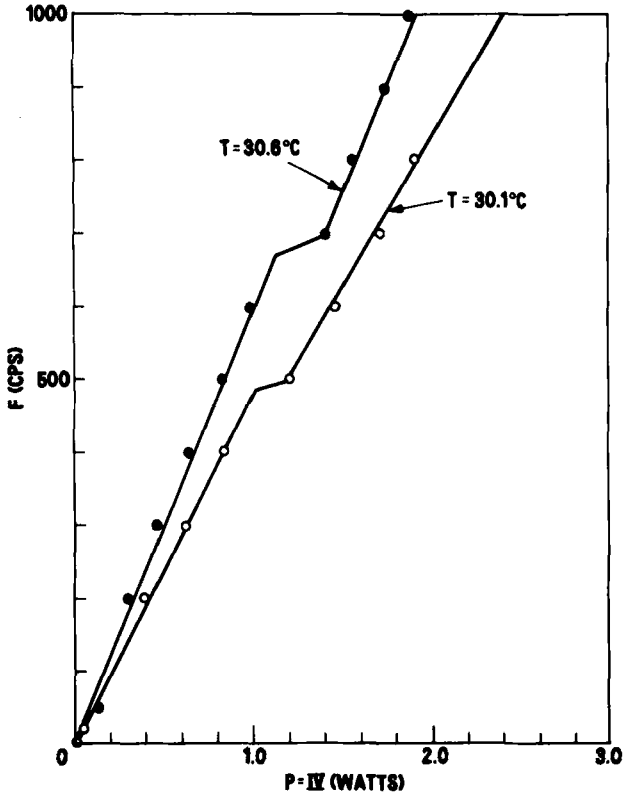


FIGURE 10 Frequency versus power to align BPI ($T = 30.1°C$) and BPII ($T = 30.6°C$) for the 50% CB15-M18 mixture. Here the sample thickness is 125$\mu$.

If $V$ is the voltage (in volts) to just unwind the cholesteric of pitch $p$ (cm) in a sample of thickness, $d$ in (cm) with twist elastic constant $K_2$ (dynes) and $\epsilon_a$ (cgs) dielectric anisotropy, then:[24]

$$\frac{K_2}{\epsilon_a} = \frac{V^2 p^2}{300^2 d^2} \cdot \frac{1}{(4\pi^5)} = 9.1 \times 10^{-9} \frac{V^2 p^2}{d^2}. \tag{3}$$

In order to estimate $K_2/\epsilon_a$ for these mixtures, we need the threshold field to just unwind the cholesteric, $V$. This field is difficult to determine owing to the vigorous circulation even in a dc field and is lower than the values shown in Figure 11. From Figure 11 we deduce an upper limit for $K_2/\epsilon_a$. This is $1.96 \times 10^{-8}$cgs units in the cholesteric phase at 29.5°C; $3.2 \times 10^{-8}$cgs units in BPI at 29.65°C; and $3.9 \times 10^{-8}$ cgs in BPII at 29.75°C. So, if $K_2$ is not too different in all these phases, $\epsilon_a$, which scales with the orientational order, is about one half of the cholesteric dielectric anisotropy in the blue phases.

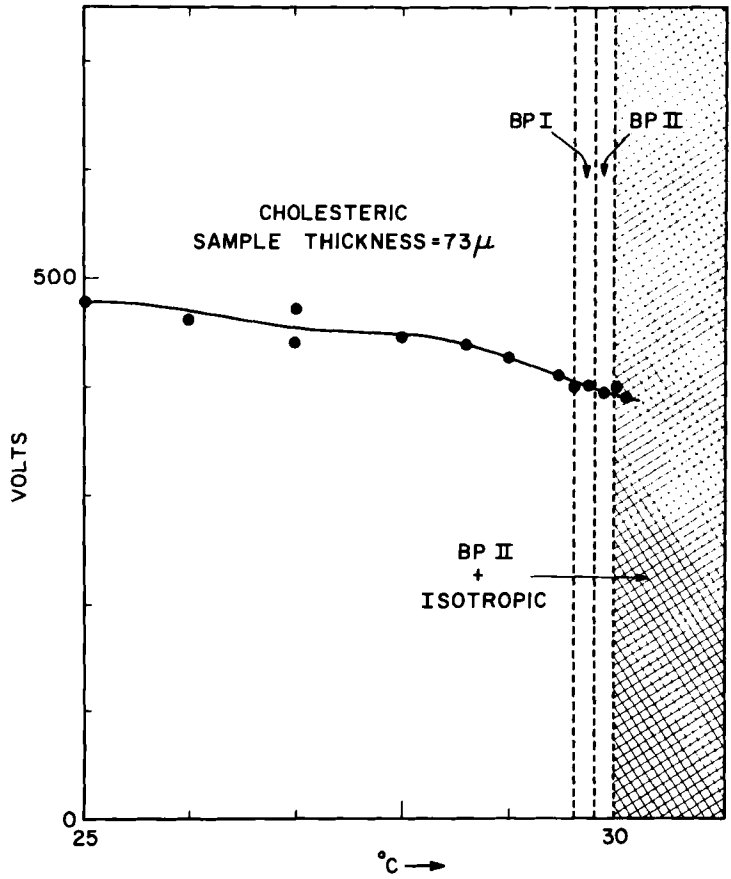


FIGURE 11 The voltage to align the director in the cholesteric, BPI and BPII phases. The voltage to unwind BPI and BPII is not very different from the value for the cholesteric phase despite the fact that the pitches in the three phases are quite different (see Figure 8). This fact further reinforces the notion that blue phases are a textural modification of the cholesteric phase.

$\epsilon_a$ for this mixture is about 10 cgs units so $K_2$ is less than $1.96 \times 10^{-7}$ dynes in the cholesteric phase.

## IV MODEL

### A General remarks

As mentioned in the introduction, our model is based on the idea that blue phases are a result of the spontaneous emulsification of the isotropic phase and the cholesteric phase. The nematic phase acts as emulsifier. Due to the extremely small temperature range over which the blue phase is stable (on the

order of .5°C or less) this hypothesis is a feasible one. In this section we discuss a possible model of the blue phase. It is constructed from non-singular spherical cholesteric units. It will be seen that these spheres will pack into a b.c.c. lattice in BPI without additional singularities. Non-singular nematic regions fill the space between the spheres. Because of the twist energy lost in these nematic regions, the radius of the isotropic regions scales with the square of the pitch. This sets an upper limit to the cholesteric pitch which can support this kind of phase. If nematic point defects are required, a lower limit is set to the pitch for BPI. The ratio of the BPI lattice parameter to the cholesteric pitch is expected to be 1.22 and the ratio of the BPII periodicity to the cholesteric is expected to be ~0.8.

### B Cholesteric spheres—the basic unit

Figure 12 shows two kinds of non-singular cholesteric spheres each of diameter, $p$ and containing a disclination loop. We also have models of singular cholesteric spheres but do not discuss them here. For the top non-singular sphere, the director configuration in spherical polar co-ordinates is:

$$n_r = -\cos\theta$$
$$n_\theta = \sin\theta\cos qr$$
$$n_\phi = \sin\theta\sin qr. \tag{4.1}$$

The Frank elastic energy of this configuration, i.e. Figure 12(a), of radius $p/2$ is

$$F = \pi p[4K_1 + 0.58K_2 + 3.9K_3] \tag{4.2}$$

where $p/p_0 = 1.22$ minimizes the twist energy at constant volume. $p_0$ is the equilibrium twist of the cholesteric in a planar texture. $K_1$ is the Frank elastic constant of splay, $K_2$ of twist and $K_3$ of bend.

An equivalent sphere is one for which

$$n_r = \cos\theta$$
$$n_\theta = -\sin\theta\cos qr$$
$$n_\phi = -\sin\theta\sin qr. \tag{4.3}$$

The bottom sphere (Figure 12) is also non-singular but of "opposite sign" to the one above it. At $p/2$, the director rotates in the opposite sense to the top sphere. We have not calculated its energy explicitly because there does not seem to be a simple way to represent its director configuration, but we can estimate it.

We know from experience with nematic point defects that in general, the positive and negative points of equal weight ($m$, say) do not have the same elastic energy—even in the one constant approximation, $K_1 = K_2 = K_3$. This is because some of the strain energy of the negative points is taken up by the

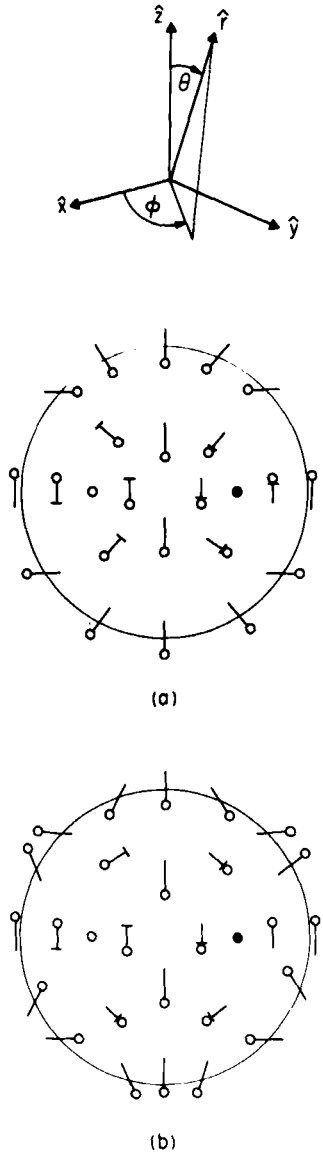


FIGURE 12 Non-singular cholesteric spheres of opposite topological sign. Inside each sphere is a disclination loop. Our co-ordinate system is shown at the top of this figure. The axis of revolution is the Z-axis. The top figure (a) is of positive sign since the director rotates in a clockwise sense when the sphere is traversed in a clockwise sense. The bottom sphere (b) is negative since its director rotates counter clockwise for a clockwise traversal of the sphere.

A cross bar indicates the end of the director which lies below the plane of the paper. A right handed cholesteric is shown here. We estimate the energy of the negative sphere (b) to be lower than that of the positive one by about 1/3. Neither sphere requires a core.

curvature of the sphere. For example, the energy for the radial point defect, ($n_r = 1$, $n_\theta = 0$, $n_\phi = 0$) is $8\pi K_1 R$ whereas for the $m = -1$ defect ($n_r = -\cos 2\theta$, $n_\theta = \sin 2\theta$, $n_\phi = 0$), it is $8\pi R/5[K_1 + \frac{2}{3}K_3]$, or in the one constant limit, 1/3 of the energy of the positive point. The differences become even more dramatic in the case of the $m = 2$ points. The energy of the $m = +2$ ($n_r = \cos\theta$, $n_\theta = \sin\theta$, $n_\phi = 0$) point is $16\pi R[\frac{2}{3}K_1 + \frac{1}{3}K_3]$, whereas for the $m = -2$ ($n_r = \cos 3\theta$, $n_\theta = -\sin 3\theta$, $n_\phi = 0$), it is $4\pi R(0.838K_1 + 1.029K_3)$ which in the one-constant limit is even less energetic than the radial point.

Notice that in the one constant limit, the energy of our non-singular cholesteric sphere is comparable to the nematic point defect $m = 2$ which its outer shell resembles. Consequently, we expect that the energy of the negative cholesteric $m = -2$ will be comparable to the nematic $m = -2$ point defect or about 1/3 the energy represented in Eq. 3. We assume that the twist energy depends upon the pitch in the same way as the positive cholesteric sphere.

No additional core energy for these cholesteric spheres need be considered.

Finally, note that the configuration in the interior of these spheres is nothing more than a disclination loop. The energy of these loops is finite and scales with the loop length, $R$. We consider the cholesteric-BPI transition one in which disclination loops unbind in BPI. We speculate that the entropy of a disclination loop will be like that of a dislocation loop,[25] i.e. $S = -kTln(g^R)$, where $R$ is the length of the loop in units of molecular length and $g$ is a constant. The total energy $E$ will then be composed of an elastic part $\sim AR$ ($A$ a constant such as found in Eq. (4.2) and an entropy part $-kTln(g^R)$ so that at sufficiently high $T$, an array of disclination loops could be a stable phase provided this does not conflict with the elasticity of the cholesteric medium (see later Section IVC3), that is, cost too much twist energy.

### C BPI

*1 Two dimensional packing* Due to the symmetry of these spherical defects, a square packing in the plane (Figure 13) is seen to be less energetic than a close packing because in the square case, at the point of contact of a sphere with its four nearest neighbors in the plane, both director orientation and twist axis are continuous. In a close packed arrangement neither are for this pair of defects—although a close packed arrangement of different spheres might work. Thus, the total energy for the square packing does not introduce additional strains at the points of contact and furthermore, the continuity of the twist axis from one sphere to another (see the bottom of Figure 13) lowers the overall twist energy when the spheres touch.

*2 Three dimensional packing* Now let's consider extending this model into the third dimension.

A simple cubic arrangement of spheres results when the next layer stacks in phase with the first. There would be a string of point defects just above (or

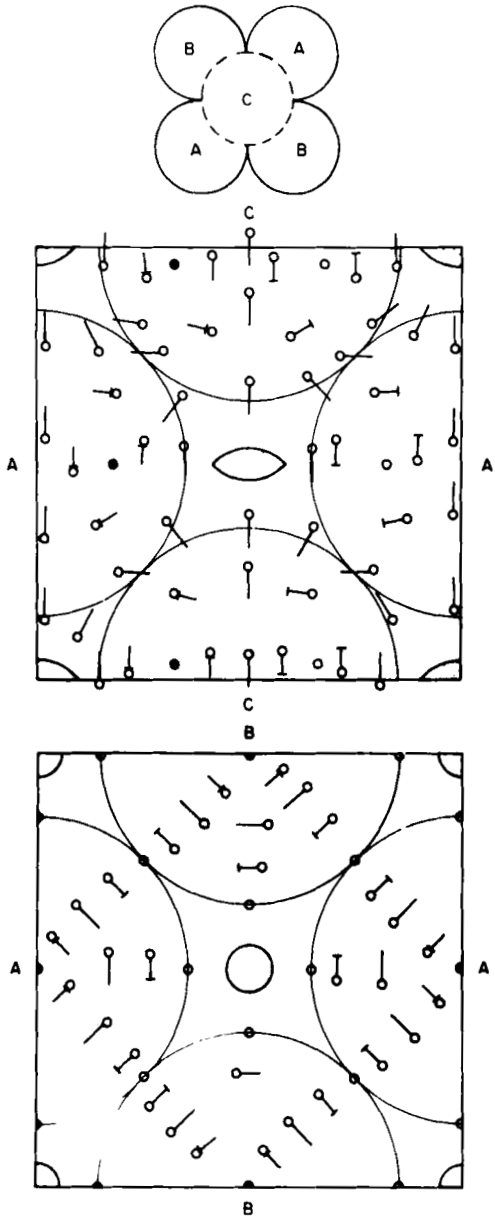


FIGURE 13 The top of the figure identifies spheres by A, B, and C arranged in a b.c.t. way. The C sphere lies above (and below) the plane containing the A and B spheres. Isotropic regions are represented by the cross-hatched regions and are shown here in the shape of round disks. In the middle figure, the director configuration is shown for the plane containing the (1,1,1) axis of a b.c.c. lattice. The bottom figure depicts the same thing for the plane containing the (1,0,0) and (0,1,0) axes. The letters beside the figures identify the spheres relative to the top diagram. By slicing down the spheres, this b.c.t. packing can be relaxed to a b.c.c. one.

below) the hatched region in Figure 13. If, on the other hand, the spheres are placed "interstitially" so that the directors and the twist axes from one row are again continuous at the points of contacts then, the spheres are arranged in a b.c.t. packing. Six spheres enclose a small nematic region which need have no singularity at all and still enclose an isotropic volume of radius, $R_{NI}$ (see top Figure 13).

By removing a small portion from the top and bottom of each sphere in Figure 12, so that they more nearly approximate toruses, the body centered tetragonal packing shown in Figure 13 can be relaxed to a b.c.c. one.

The actual shape of the isotropic region can even distort (as we have shown in the figure) to accommodate the particular boundary condition without necessitating a singularity. Here it is shown as disc-like to accommodate a homoeotropic orientation. An ellipsoid of revolution might be better for a homogeneous orientation.

Now the energy density of the spheres depends upon their size. This is shown in Figure 14 for non-singular spheres (Eq. 4) as a function of the sphere size in units of $p$, the pitch. A single positive sphere, of radius $R = 0.5p$ is near a relative maximum compared to a sphere of $R \sim .3p$. The gain in elastic energy from a b.c.c. packing of many spheres equal to the half pitch compared to a packing of spheres of nearly half this radius converts a relative maximum energy configuration for a single sphere to an energy minimum for many spheres. But, once there is no longer a topological reason to maintain this sphere size (because now the spheres are no longer connected by a mesophase) they shrink to the relative minimum shown in the graph.

In the first case, (our model for BPI), $p/p_0$ which minimizes the twist energy is 1.22 which compares very well with the observed values $1.15 \leq a_{\text{BPII}}/p_0 \leq 1.25$ [Section IIIB2].

*3 The nematic interstices* A three-dimensional packing such as shown in Figure 13 implies that in a volume $(4/3)\pi(R_{NC}^3 - R_{NI}^3)$, where $R_{NC}$ is the effective maximum radius of the nematic regions and $R_{NI}$ is the effective radius of the isotropic region, $K_2 q_0^2/2$ in twist energy is lost. To create an isotropic region of volume $\frac{4}{3}\pi R_{NI}^3$ requires $(L/T)\Delta T$ ergs/cm$^3$/°C where $\Delta T$ is the difference between the clearing temperature and the ambient temperature. A nematic-isotropic interface of radius $R_{NI}$ requires $4\pi\sigma R_{NI}^2$ ergs where $\sigma$ is the nematic-isotropic interfacial energy $\sim 2 \times 10^{-2}$ ergs/cm$^2$.[26] To minimize the loss in twist energy $R_{NI}$ should be big but to minimize the loss in interfacial energy $R_{NI}$ should be small. A minimum occurs when

$$R_{NI} = \frac{4\sigma}{q_0^2 K_2 - 2(L/T)\Delta T}. \tag{5}$$

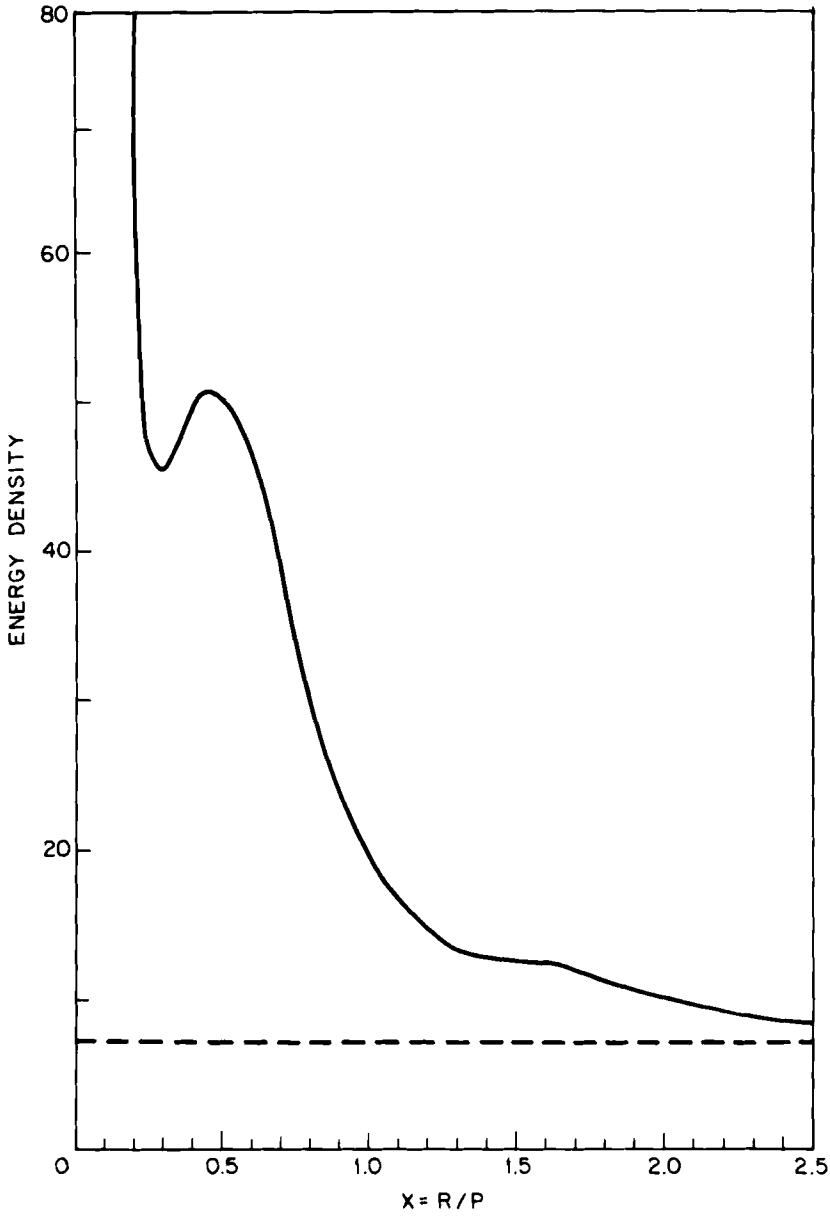


FIGURE 14 Energy density of the non-singular sphere shown in Figure 12(a) versus the sphere radius, $R$, in units of pitch. When $R/p = x = 0.5$, the ratio of the pitches in this configuration compared to a planar texture is 1.22. When $x = 0.3$ (the relative minimum), this pitch ratio is 1.49. BPI occurs in the former case. Should the radius shrink to $x = .3$, a less energetic configuration is an untwisted cholesteric in an $m = +1$ point defect configuration (see Figure 15).

(a) For $R_{NI} > 0, K_2 q_0^2 > 2(L/T)\Delta T$. This determines the temperature range of the blue phase. For our sample of CP, $T_{CI} \cong 113°C$. (Figure 3). A similar sample with this $T_{CI}$ gives $L/T = 1.9 \times 10^4 \text{ergs/gm/°K}$.[27] This is an upper limit since part of the entropy is due to a substantial specific heat anomaly. Taking $q_0 = 20 \times 10^4 \text{ cm}^{-1}$ (Figure 5) and $K_2 = 2 \times 10^{-7}$ dynes, the value we measured in the CB15-6OCB mixture, the expected blue phase range is $\Delta T < .21°C$. We in fact measure a blue phase range of $\Delta T \sim 0.2$ for CP (Figure 4). Thus, Eq. (5) underestimates the blue phase range slightly perhaps due to the fact that $L/T$ is *overestimated* and/or $K_2$ for CP is larger. Still the agreement is not too bad.

(b) When $R_{NI} \gtrsim p/2$, it is unlikely that an emulsion solution will be stable. This sets an upper limit to the cholesteric pitch which can sustain a stable intermediate colloidal phase. We consider the limit when $K_2 q^2 \gg 2(L/T)\Delta T$. In the case of the CB15-6OCB mixtures, $K_2 \sim 2 \times 10^{-7}$ dynes (see III), $\sigma \sim 2 \times 10^{-2} \text{ dynes/cm}^2$, and $R_{NI} \gtrsim p/2$ (taking $p \sim p_0$) for $p/2 \geq 2500\text{Å}$ in remarkably good agreement with the observed value of 2100Å (see Figure 6).

This is about the same number found in Ref. 10 for a different system. Thus the most probable materials to exhibit an infra-red or visible blue phase, i.e. one in which the lattice parameter is resolvable in the optical microscope, will have a large $K_2$ and a small $\sigma$.

If there are topological constraints which entail a nematic point defect, then

$$R_{NI} = \frac{2(\sigma \pm \sqrt{\sigma^2 - K_1 K_2 q^2})}{q^2 K_2}, \quad \Delta T \sim 0. \tag{6}$$

This sets a lower limit to the pitch for BPI of 1500Å for the same values of the material constants as above. The fact that CB15 has a blue phase which for thermodynamic reasons (see the Introduction) we believe is BPI, argues in favor of non-singular nematic regions in this case since its cholesteric half-pitch (650Å) is below 750Å, the minimum to stabilize BPI.

### D BPII and BPIII (blue fog)

As the amount of isotropic liquid increases, the sphere radius shrinks towards the relative minimum shown in Figure 14 and the nematic boundary condition becomes increasingly incompatible with a bulk twist.

A cholesteric sphere of radius $R_{MAX} \sim p/2$ twists and its elastic energy is comparable to nematic spheres of the same radius with point singularities of the same strength, $m$. The energy to untwist a cholesteric scales with $R_{MAX}^3$. But, for cholesteric spheres of radius $R_{MAX} \sim p/4$, the amount of twist energy it costs becomes negligible compared to the gain that can be made by stepping down the sphere configuration from an $m = \pm 2$ to an $m = +1$ required by the spherical nematic boundary condition.

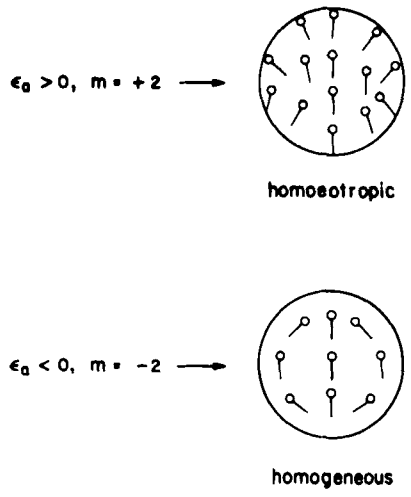


FIGURE 15 When $\epsilon_a > 0$, the director at the cholesteric-isotropic interface is homoeotropic. When the radius of the positive sphere (top Figure 12) shrinks to $p/4$, it can accommodate these boundary conditions. The interior of the negative sphere fits homogeneous boundary conditions. These are expected to prevail when $\epsilon_a < 0$. Only diametral sections of both spheres are shown.

In general, the relative orientation of the spheres is randomized by Brownian motion so there will be no net birefringence. BPII, then, is a kind of plastic crystal. On the other hand, when a symmetry axis is imposed by surface treatment, as in the Cano wedge, for example, at least those spheres in contact with the surface will all be oriented the same way. In general, there are always two sets of platelets; one set on the top substrate and the other, on the bottom substrate.

The inner half of each of the spheres shown in Figure 12 is suitable for one of the two "canonical" boundary conditions: (1) homogeneous, where the director lies in the interface and (2) homoeotropic, where it is perpendicular. This is shown in Figure 15.

In the homoeotropic case, the $m = -2$ spheres no longer exist in BPII because they cannot meet the constraint of homoeotropic boundary conditions. In a similar way, in the homogeneous case, the $m = -2$ spheres survive the transition to BPII and become $m = +1$ spheres but the $m = +2$ spheres do not.

In both cases, the sphere radius is on the order of $p/4$ and consists of untwisted cholesteric. If the spheres are separated by a radius width of isotropic liquid (i.e. $p/4$), then the lattice parameter $a_{BPII}/p_0 \sim 0.75 p_0$ in agreement with the observed value. It may be somewhat larger or smaller depending upon the amount of isotropic liquid between spheres. In order to account for the small optical rotatory power in BPII, each sphere may be twisted with respect to neighboring spheres or, perhaps, the cholesteric inside each sphere is slightly

twisted. From experience with large pitch cholesteries, this latter seems less likely since the sphere size is small compared to the pitch and the boundary conditions at the sphere surface are nematic-like.

This model for BPII bears some slight resemblance to the nematic-like cholesteric "blobs" of Toner and Nelson.[25]

The blue fog is then just a decoupled arrangement of cholesteric spheres. This agrees with Marcus'[4] idea that the blue fog is a liquid like phase whereas BPI and BPII are solid-like. A dense random packing of hard spheres coupled by long range van der Waal's forces would account for the single reflection seen in the blue fog.[28]

### E Cano wedge

In the Cano wedge, the spheres must satisfy two different boundary conditions: (1) at the glass surface and (2) at the cholesteric-isotropic interface.

In the case of the 6OCB-CB15 mixtures, these conditions are: homoeotropic at the interface and homogeneous at the glass surface. Thus in BPII, hemispheres nucleate at the glass interface and they tend to be close packed. A planar nematic at the glass interface would have to bend to satisfy the additional homoeotropic boundary condition at the isotropic interface. Therefore, in this latter case, only one kind of sphere can be at the surface in BPII. This forces a (1,0,0) habit for BPII. When the $m = -2$ defects are added (see Section D above), the center of the $m = +2$ spheres are oriented along (1,0,0) giving rise to the (2,0,0) reflections in b.c.c. Only the lattice parameter is about 35% smaller in BPII than it is in BPI.

For the S1014-CE2 mixtures, the boundary condition is homogeneous at the glass surface and the isotropic interface. $\epsilon_a < 0$ for S1014 and the dipole associated with the cyano group is perpendicular to the director. Since this is compatible with a planar nematic, rather than hemispheres, a thin layer of nematic is at the glass isotropic interface which will tend to orient the nearest layer of spheres so that their axes lie parallel to the director on the glass as shown in Figure 16. A slightly repulsive long range van der Waal's interaction would prevent a closest packed arrangement resulting in a (1,1,0) habit. In the homogeneous case, the (1,1,0) planes of the b.c.c. structure are the (1,1,0) planes of the simple cubic structure after addition of the $m = +2$ points (Figure 16).

Once a well ordered surface layer is formed, the long range van der Waal's forces[29] could become strong enough to orient all the spheres so that the "twinkling," a symptom of long range orientational correlations, can often be observed in BPII. If the long range van der Waal's forces are strong enough to overcome the disorienting effect of Brownian motion, a very well ordered BPII could be weakly birefringent.

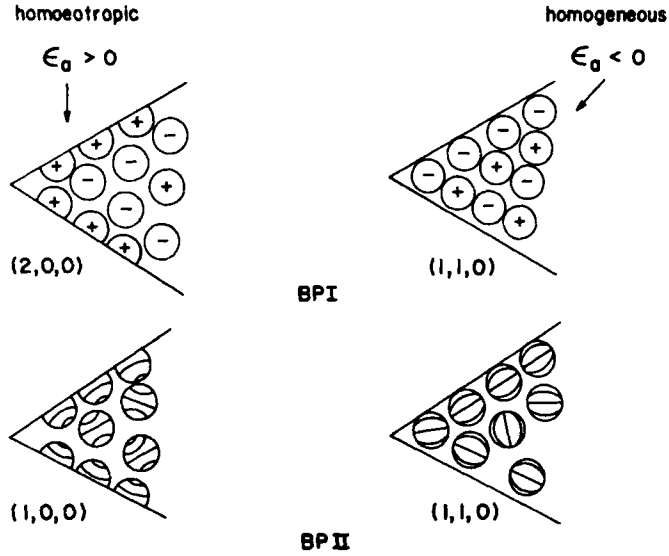


FIGURE 16 Since the Cano wedge lines are nucleated from BPII, the habit of BPI will be related to the habit of BPII. Thus $\epsilon_a > 0$ will have a different habit from $\epsilon_a < 0$ materials when homogeneous boundary conditions are imposed. This is depicted in the rest of the figure where the positive defect of BPI is shown in the top of Figure 12 and the negative one in the bottom of Figure 12. The kind of nematic-like $m = +1$ in BPII is determined by the cholesteric-isotropic boundary condition and they are shown in Figure 15.

### F Cholesteric spheres in a field

At fields below the value to unwind them, the spheres of BPI will reorient with the twist axis perpendicular to the field. Since the twist axis is essentially toroidal, this will be hard to do—accounting in part for the extraordinary stirring activity we observe even in small dc fields. With a large enough field, the spherical symmetry will be destroyed and gradually the birefringence will be restored (as we observe). Once we destroy the spherical shell, the pitch will tend to revert back to its planar value (rather than the inflated value demanded by the loop geometry), i.e., Figure 12. This accounts for why the critical field does not seem to be too different in the cholesteric and blue phase regions. Effectively, we have transformed BPI back to the same cholesteric it came from, i.e., applying the electric field released the cholesteric from its cage.

As the BPII spheres orient in the field the birefringence increases, however, once they are aligned so that the director is parallel to the field, which they can do without introducing singularities, the birefringence is again zero. Since the diameter of the sphere is on the order of $p_0/2$, the field strength need only be enough to penetrate the spheres. If a magnetic field, rather than an electric

field could be used, it would probably be apparent that this process is a continuous one once the magnetic coherence length is small enough to fit into the spheres.



## CONCLUSIONS

We have determined phase diagrams (using the light microscope) and pitch (using a wedge geometry) for cholesteryl propionate mixed with various nematics and a chiral nematic mixed with cyanohexyloxybiphenyl (6OCB). We have succeeded in untwisting both blue phases of this latter mixture in an electric field. We find that with increasing field, BPI transforms to a cholesteric before it becomes aligned in the field whereas BPII transforms to a nematic before it aligns in the field. Furthermore the voltage to align blue phases is not very different from that in the cholesteric phase.

We have presented a model of the blue phase which accounts for all of the salient features of the blue phases:

1. The extremely narrow temperature range of blue phases (Section IB).
2. The possibility of three blue phases: BPI, BPII and the blue fog and how they are related (Section IB and IV).
3. The occurrence of only one blue phase in very pure materials (Section IB).
4. The magnitude of the lattice parameter relative to the equilibrium pitch, $p_0$ of BPI and BPII given a b.c.c. and s.c. structure respectively (Section IVC2 and IVD).
5. The orientation habit of the blue phases in the Cano wedge for both $\epsilon_a > 0$ and $\epsilon_a < 0$ materials (Section IVE).
6. The isotropy of BPI and BPII with the possibility that for large enough oriented samples, BPII could become anisotropic (Section I and IVE).
7. The "twinkling" frequently observed in oriented samples of BPII (Section IVE).
8. The maximum pitch for which blue phases can occur (Section IVC3).
9. The continuity of the voltage to untwist the cholesteric, BPI and BPII phases (Section IVF).
10. The fluidity of blue phases (Section B3).

In our model, blue phases are triggered by the appearance of submicroscopic isotropic regions in the cholesteric. These regions necessitate nematic boundary conditions at the isotropic interface. Because cholesterics and nematics are thermodynamically the same phase, they are miscible (*their* interfacial energy is effectively negative), and a cholesteric isotropic emulsion occurs to minimize

the loss in twist energy. The nematic is the emulsifier. The inside phase is isotropic and the outside phase is cholesteric in a defect loop configuration. We speculate that the entropy associated with disclination loops could stabilize this phase provided the pitch is small enough. But a cholesteric caged by untwisted regions and confined to a volume whose radius is a half pitch, is effectively a nematic. Increasing the temperature results in the emulsion turning inside out so that cholesteric is the inside phase and the isotropic liquid the outside one. This is BPII. The maximum pitch of the cholesteric which can sustain a blue phase arises because the size of the isotropic regions scales with the square of the pitch. We have constructed a director model which provides additional support for a b.c.c. structure for BPI and a simple cubic structure for BPII. On the other hand, our model does not preclude the possibility of an f.c.c. BPI[6] and BPII when the topology of the "basic sphere" is changed due to the exigencies imposed by external constraints.



## Acknowledgments

We thank M. Marcus for stimulating discussion and R. Filas for providing us with Refs. 20 and 21. One of us (P. L. F.) thanks W. Heffner for useful conversations.

## References

1. H. Stegemeyer and K. Bergmann in "Liquid Crystals of One and Two-Dimensional Order," W. Helfrich and G. Heppke, editors, Springer-Verlag (New York, 1980), p. 174.
2. D. Armitage and F. P. Price, *J. Appl. Phys.*, **47**, 2735 (1976); E. M. Barrall, R. S. Porter and J. F. Johnson, *Mol. Cryst.*, **3**, 103 (1967); H. Arnold and P. Roediger, *Z. Phys. Chem.*, **239**, 283 (1968); K. Bergmann and H. Stegemeyer, *Z. Naturf.*, **34a**, 251 (1979).
3. S. Meiboom and M. Sammon, *Phys. Rev. Letters*, **44**, 882 (1980).
4. M. Marcus, *Journale de Physique*, **42**, 61 (1981) and P. L. Finn (unpublished).
5. D. L. Johnson, J. H. Flack and P. P. Crooker, *Phys. Rev. Letters*, **45**, 641 (1980).
6. A. J. Nicastro and P. H. Keyes (to be published).
7. M. Marcus, (to be published).
8. S. Meiboom and M. Sammon (to be published).
9. Terence K. Brog and Peter J. Collings, *Mol. Cryst. Liq. Cryst.*, **60**, 65 (1980).
10. P. H. Keyes, A. J. Nicastro and E. M. McKinnon, *Mol. Cryst. Liq. Cryst.* (in press).
11. S. A. Brazovskii and S. G. Dmitriev, *Zh. Eksp. Teor. Fiz.*, **69**, 979 (1975); *Soviet Physics JETP*, **42**, 497 (1976).
12. S. A. Alexander and P. G. deGennes presented at the European Conference on Smectics, Madonna di Campiglio, Italy, January (1978).
13. G. Sigaud, *Mol. Cryst. Liq. Cryst. Letters*, **41**, 129 (1978).
14. R. M. Hornreich and S. Shtrikman, *J. Physique (Paris)*, **41**, 335 (1980).
15. W. Kuczynski, K. Bergmann and H. Stegemeyer, *Mol. Cryst. Liq. Cryst. (Letters)*, **56**, 283 (1980).
16. See for example, A. E. Stieb, *Journale de Physique*, **41**, 961 (1980); W. E. L. Haas and J. E. Adams, *Appl. Phys. Letters*, **25**, 535 (1974).
17. P. E. Cladis, A. E. White and W. F. Brinkman, *Journale de Physique*, **40**, 325 (1979).
18. A. Saupe, *Mol. Cryst. Liq. Cryst.*, **7**, 59 (1969).
19. I. G. Chistyakov and L. A. Gusakova, *Soviet Physics Crystallography*, **14**, 132 (1969).
20. Albert Axman, *Z. Naturforschg.*, **1a**, 615 (1966).

21. R. Hareng (private communication to M. Cohen, P. Pieranski, E. Guyon and C. D. Mitescu cited in *Molecular Crystals*, **38**, 97 (1977)).
22. R. Cano, *Bull. Soc. Franc. Mineral.*, **91**, 20 (1968).
23. W. Helfrich, *Appl. Phys. Letters*, **17**, 531 (1970); H. Miike, T. Kohno, K. Koga and Y. Ekina, *J. Phys. Soc. Japan*, **43**, 727 (1977).
24. R. B. Meyer, *Appl. Phys. Letters*, **12**, 281 (1968); P. G. deGennes, *Solid State. Comm.*, **6**, 163 (1968).
25. We thank D. R. Nelson for a discussion on this point. See John Toner and David R. Nelson, *Phys. Rev.*, **B23**, 316 (1981); W. Helfrich, *J. Phys.* (*Paris*), **39**, 1199 (1978).
26. D. Langevin and M. A. Bouchiat, *CRAS*, **B277**, 731 (1973).
27. E. M. Barrall and J. F. Johnson in "Liquid Crystals and Plastic Crystals," edited by G. W. Gray and P. W. Winsor (Wiley, New York, 1974), Vol. II, p. 254.
28. M. Marcus (private communication).
29. P. G. deGennes, *CRAS*, **B271**, 469 (1970).